9

EXPLORER SATELLITES LAUNCHED BY JUNO 1 AND JUNO 2 VEHICLES

J. Boehm, H. J. Fichtner, and Otto A. Hoberg

Astrionics Division
George C. Marshall Space Flight Center
National Aeronautics and Space Administration
Huntsville, Alabama

In the early 1950's rocket technology had advanced to such a state of the art that a project for orbiting an artificial moon around the Earth became feasible. At that time Dr. Wernher von Braun--well cognizant of this situation--began to shape solutions for the realization of the satellite concept. His great ability to combine ingenious fantasy with realistic engineering thinking was set forth in the paper "A Minimum Satellite Vehicle Based on Components Available from Missile Development of the Army Ordnance Corps, Guided Missile Development Division, Ordnance Missile Laboratories" [1]. This report contains the basic scheme for the Juno 1 and Juno 2 vehicles.

The efforts and planning for a satellite mission resulted in the first U. S. satellite project, Orbiter. The Vanguard, a purely scientific project, soon succeeded the Orbiter. In parallel to the Vanguard program a multistage rocket system, known as Jupiter C, was developed by the Army in Huntsville, Alabama, under Dr. von Braun's direction, for the investigation of reentry nose cones. Satellite capabilities were also inherent in this vehicle which, when somewhat modified, was used to place the first U. S. satellite in orbit on January 31, 1958 (only 84 days after the order was given).

This chapter covers the development of Explorer satellites and is preceded by a brief discussion of the carrier vehicles and their satellite lifting capabilities. General design objectives which were of essential influence to the layout of the mechanical satellite systems are presented. Miniaturization of components, lightweight structure, and utmost design symmetry were necessary because of the low payload capabilities and the spin applied to the upper stages.

Consideration is given to the dynamics involved to maintain prescribed orientation of the satellites in orbit. It is shown how the satellite program produced many new problems in the field of instrumentation, tracking, design, and systems engineering. Another part of this

chapter deals with the power supply systems, the electrical networks, and the timing devices applied in the satellites. Particular emphasis is given to the solution for solar cell battery power supply systems.

The concluding part refers to the broad and thorough test program which helped to achieve the indispensable reliability necessary for space missions.

9.1 The Carrier Vehicles

The Juno 1 and Juno 2 vehicles, both four-stage rocket systems, were conceived as fast and thrifty solutions for launching satellites and space probes. Both were developed by the former Development Operations Division of the Army Ballistic Missile Agency (contributing the first stages, guidance and control systems, and the launching) and by the Jet Propulsion Laboratory (contributing the high-speed upper stage assembly).

The composition of these multistage carrier vehicles was characterized by the choice of thoroughly proven components. It was intended that required modifications of existing hardware would not impair the reliability of the vehicles. Thus it became possible to provide, with existing means, a workable rocket system carrying payloads ranging from a maximum of 25 lb for Juno 1 to a maximum of 92 lb for Juno 2 (Table 9.1). Both vehicles evolved from the Jupiter C, a composite reentry test vehicle developed by the Army for investigating the aerodynamic heating of missile nose cones when diving into the Earth's atmosphere. The main difference between Juno 1 and Juno 2 was in the first stage (Figs. 9.1 and 9.2). Juno 1's main stage was a modified Redstone ballistic missile while a modified version of the more powerful Jupiter ICBM was Juno 2's main stage.

Both vehicles had the same arrangement of high-speed solid propellant stages. Their second stages were powered by 11 solid propellant motors, and the third stages consisted of three such motors; a single motor was used on their fourth stages. The payload was attached directly to the top of the fourth stage. The high-speed stage motors were clustered symmetrically about the longitudinal vehicle axis and housed in a cylindrical launcher. With a concentrically arranged shaft, this launcher could rotate in ball bearings, supported by the forward end of the first stage instrument compartment. Spinning of the high-speed stages was mandatory to minimize slight thrust differences between the motors. A shroud was introduced for the Juno 2 vehicle for protection from greater aerodynamic heating during the ascending part of the trajectory and for support of an angle-of-attack meter located in front.

Table 9.1 Data Pertaining to Launched Satellites

Satellite	Vehicle	Firing Date	Perigee	Apogee	Eccentricity	Inclination (deg)	Period (min)	Weight Without 4th Stage	Initial Spin (rpm)	Orientation Required	Separation of 4th Stage
Explorer 1	Juno 1	Jan. 31, 1958	360	2552	0.139	33.2	114.7	18.1	750	none	none
Explorer 2	Juno 1	Mar. 5, 1958	----------					18.1	750	none	none
Explorer 3	Juno 1	Mar. 26, 1958	195	2810	0.166	33.4	144.7	18.1	750	none	none
Explorer 4	Juno 1	Jul. 26, 1958	267	2219	0.128	50.3	110.1	25.8	750	none	none
Explorer 5	Juno 1	Aug. 24, 1958	----------					25.8	750	none	none
Beacon 1	Juno 1	Oct. 22, 1958	----------					28.5	---	none	none
Payload AM-16	Juno 2	Jul. 16, 1959	----------					87.5	---	yes	yes
Payload AM-19B	Juno 2	Aug. 14, 1959	----------					26.0	600	none	none
Explorer 7	Juno 2	Oct. 13, 1959	555	1091	0.037	50.4	101.2	92.3	425	yes	yes
Payload AM-19C	Juno 2	Mar. 23, 1960	----------					22.5	525	none	none
Explorer 8	Juno 2	Nov. 3, 1960	420	2295	0.121	49.9	112.7	87.7	445	yes	yes
Payload AM-19F	Juno 2	Feb. 24, 1961	----------					75	---	yes	yes
Explorer 11	Juno 2	Apr. 27, 1961	490	1799	0.087	28.8	108.1	85	390	yes	none
Payload AM-19G	Juno 2	May 24, 1961	----------					75	460	yes	yes

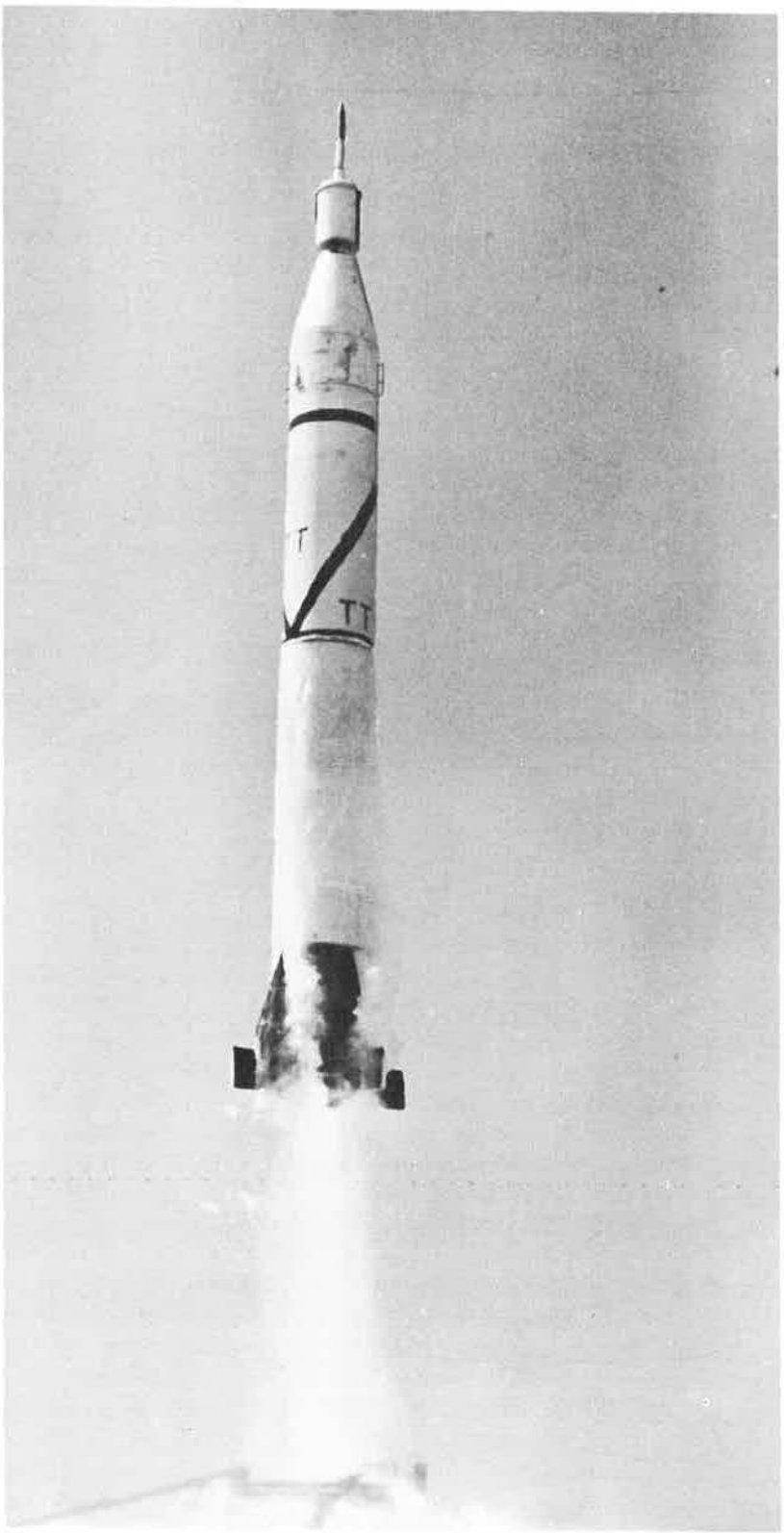

Fig. 9.1 Juno 1 configuration.

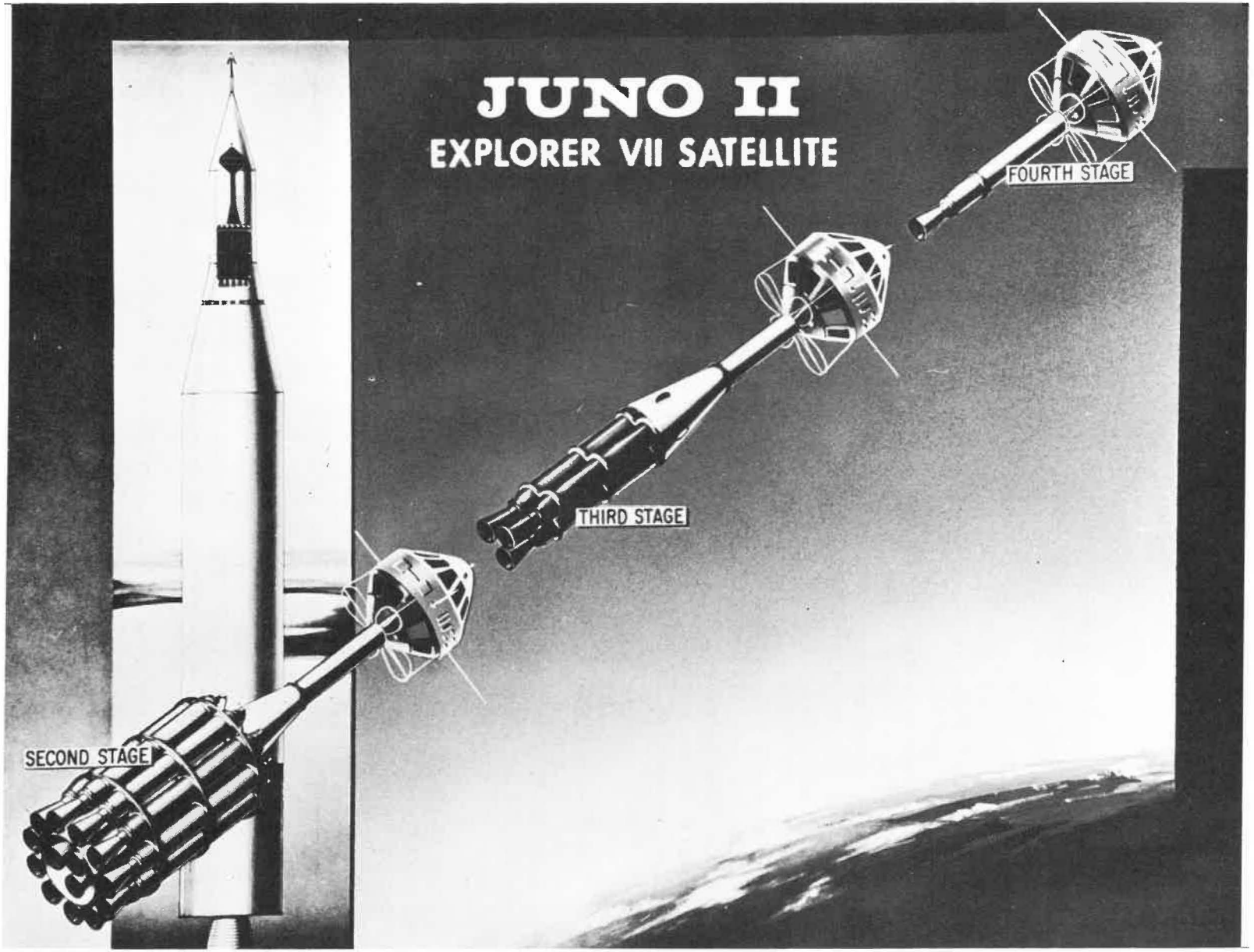

Fig. 9.2 Juno 2 vehicle and stage separation.

The flight patterns of both Juno vehicles were quite similar. The multistage rocket first rose vertically and then was tilted into the trajectory during the burning time of the first stage. Then, the instrument compartment and the launcher with the clustered upper stages were separated shortly after burnout.

To avoid bumping or other impairment of the first stage with the separated high-speed stages, the main stage was slowed down and displaced to one side by "kick" rockets. A few seconds after separation, the cone-shaped upper part of the shroud was detached by explosive bolts and springs. Again by kick-rocket action, the cone was moved sidewise to clear the path for the upper stages. During the coasting flight that followed, the instrument compartment with the spinning cluster launcher was being tilted to align the main axis of the system to a nearly horizontal position at apex. The tilting was imparted to an assembly with the spinning launcher and upper stages acting as a giant gyro [2]. During coasting flight, the attitude control was achieved by four pairs of air-jet nozzles with variable thrust. These nozzle pairs were properly arranged on the aft end of the instrument compartment. The ignition of the second stage was actuated by the program device in the first stage. The firing of the third stage followed approximately 9 sec later, and after the same interval, the fourth stage was ignited. In cases where separation of the payload from the empty shell of the fourth stage was required, a special separation device was inserted between payload and fourth stage.

The Juno 1 program began with the launching of Explorer 1 on January 31, 1958, and ended on October 22, 1958 with an attempt to launch Beacon 1. Pioneer 3, a space probe, launched on December 6, 1958, was the first flight of the Juno 2 series. The launching of payload AM-19G on May 24, 1961 completed this series (Table 9.1).

An optimum staging was not inherent in both vehicle types. Time and costs established limitations. Excessive static and dynamic accelerations of the upper stages imposed severe problems upon the payload developer. It was extremely difficult to fulfill the injection requirements for exact orbits since the amount of the spin speed of the cluster could not be chosen as high as desirable because of definite limitations prescribed by the overall configuration of this four-stage rocket.

Nevertheless, expectations were met that confirmed hopes for the Juno 1 and Juno 2 vehicles. The most significant accomplishment was the launching of the free world's first satellite.

9.2 The Mechanical System of the Satellites and Their Layout

The satellites were engineered to provide suitable structures for the great variety of scientific experiments presented by the different missions (Table 9.2). The rather low payload lifting capabilities of

Table 9.2 Satellite Missions

Satellite	Scientific Experiments On Board	Results
Explorer 1 (RS-29)	1. Cosmic ray experiment. Cosmic ray intensity surrounding the Earth's atmosphere is measured by counter. 2. Micrometeoriod experiment. Statistical distribution of the space density and the momentum of micrometeoroids is measured by means of an impact microphone and an arrangement of fracturable wire erosion gages. 3. Temperature measurements. At four typical locations to check the effeciveness of passive temperature control (surface coating).	Successful
Explorer 2 (RS-26)	Equipped like Explorer 1, but with a tape recorder for cosmic ray data storage.	Failed
Explorer 3 (RS-24)	Equipped like Explorer 1, but with a miniature tape recorder for storage and interrogation of cosmic ray data and without impact microphone.	Successful
Explorer 4 (RS-44)	Radiation experiments. Two Geiger-Mueller counters and two scintillation counters.	Successful
Explorer 5 (RS-47)	Similar to that of Explorer 4.	Failed
Beacon (RS-49)	High-altitude atmospheric density experiment. Evaluation by observation of the orbital characteristics. Orbit to be as circular as possible.	Failed
Payload AM-16	1. Cosmic ray experiment. For monitoring of total cosmic ray intensity, geomagnetically trapped corpuscular radiation, and solar protons by two Geiger-Mueller counters. 2. Lyman-Alpha and X-ray experiments for monitoring of the intensity of ionizing radiation striking the Earth's atmosphere by means of two specially designed gas ionization chambers.	Failed

Table 9.2 (continued)

Satellite	Scientific Experiments On Board	Results
	3. Thermal radiation balance experiment. To determine the driving force behind the circulation of the atmosphere. Measurements of three components of radiation: (1) incident radiation from the Sun; (2) reflected sunlight which never enters the Earth's thermodynamic system; (3) infrared heat radiation from the Earth and its atmosphere and measuring the temperatures of various bolometers. 4. Heavy primary cosmic ray experiment. For monitoring the heavy nuclei content of the primary cosmic radiation by argon filled ionization chamber. 5. Micrometeorite penetration experiment. To measure micrometeorite penetration and molecular sputtering by means of photo conducting CdS cells. 6. Temperature measurements. 7. Unprotected solar cell experiment.	
Payload AM-19B	High-altitude atmosphere experiment. To find the characteristics of the upper atmosphere by an orbiting 12-ft diameter inflatable sphere and beacon.	Failed
Explorer 7	Repetition of Payload AM-16	Successful
Payload AM-19C	Van Allen radiation belts experiments. To study the radiation composition, nature of the penetrating components and energy spectrum of the less penetrating components, and total energy flux in the trapped region.	Failed
Explorer 8 (AM-19D) (S-30)	Direct ionosphere measurements experiment. To study the characteristics of the ionosphere by means of onboard detectors.	Successful

Table 9.2 (continued)

Satellite	Scientific Experiments On Board	Results
Payload AM-19F (AM-19F) (S-45)	Indirect ionosphere measurements experiment. To study the characteristics of the ionosphere by propagating signals through the ionosphere.	Failed
Explorer 11 (AM-19E) (S-15)	Gamma ray astronomy experiment. To detect the high-energy gamma rays and to measure the ratio between reflected (by Earth's atmosphere) and nonreflected high-energy gamma rays by means of a gamma ray telescope capable of discriminating against neutron interaction and charged cosmic ray particles.	Successful
Payload AM-19G (S-45)	Similar to that of Payload AM-19F	Failed

the carrier vehicles forced design from the very outset toward miniaturization of components and extremely lightweight satellite structure. This apparent disadvantage offered a unique opportunity to develop sophisticated payloads with increased reliability [3, 4].

By following this prescribed development philosophy, the design was shaped by consideration of a series of parameters emanating partly from the various mission objectives and partly from the multistage carrier vehicles. Requirements for mission objectives included satellite orientation in space, appropriate mounting possibilities for the sensors, sufficient area for solar cell arrays, temperature control, and antenna arrangements. The first stage system subjected the satellites to high static, dynamic, and centrifugal accelerations. Weight limitation prohibited excessive balancing weights; therefore, the satellites had to be designed as symmetrical as possible about the spin axis. The shell of the satellites for the Juno 1 vehicles took the aerodynamic heating, since the payload was not covered by a protective shroud.

Several satellites required maintaining the spin axis as established at injection for scientific experiments and antenna orientation (Table 9.1), accomplished by spin-stabilization. Because of weight and power limitations, the use of an active attitude-control system was eliminated. An oblate inertia distribution about the spin axis was chosen to assure stable orientation of the satellite during energy dissipation. To nullify nutation, special damping was artificially introduced. The antenna systems, with their long flexible elements, lent themselves very favorably to the generation of additional nutation damping. Spin stabilization was achieved this way for Explorers 7, 8, and 11. The moment of inertia ratio with respect to the spin axis and a lateral axis through the center of gravity was 1.24:1 for Explorer 7, 1.32:1 for Explorer 8, and 1.44:1 for payload AM-19F*. These ratios were realized by separating the empty shell of the fourth-stage motor from the satellite body (Table 9.1).

The orientation of the spin axis can be preserved only under the assumption that no external torques are acting on the satellite. This assumption does not fully correspond to the actual conditions. The perturbing torques resulting from such forces as magnetic induction and differential gravity will produce a slowly increasing deviation from the original orientation of the spin axis. The rate of change is hard to predict. It is anticipated that the orientation change can be established to a reasonable degree of accuracy by comparison of the analytical results with corresponding satellite orientation measurements.

---

* Indirect ionosphere measurement satellite, which failed to orbit.

Another interesting dynamical task was offered in the spin reduction of Explorer 8 [5, 6]. The initial spin of 445 rpm had to be reduced to approximately 25 rpm to ascertain proper operation of the experiments. For maximum spin lifetime, the spin was to be reduced while full angular momentum was conserved. This could have been accomplished solely by attaching masses to the ends of the ends of the extensible dipole antenna, thereby diminishing the rpm by increasing the moment of inertia. Since weight limitation prohibited this solution, a two-step rpm reduction was applied, presenting an optimum compromise between weight penalty and loss of angular momentum. The concept chosen for the first phase consisted of two wires wound around the circumference of the satellite in a direction opposite of the direction of the spin (Fig. 9.3). Masses were connected to the outer wire ends and the wires were allowed to unwind. When completely unwound, the wires were released to allow a reduction to 100 rpm. The second step brought a spin reduction from 100 rpm to approximately 25 rpm. The second reduction was obtained by a combined antenna-release and de-spin system, which applied a special braking device to control the unreeling velocity of the wires.

A particularly intriguing dynamic problem occurred with the orientation requirement for Explorer 11. The satellite was placed into orbit with a spin velocity of 390 rpm about the minimum moment of inertia axis. The mission demanded a transfer of the spin about this axis to spin about the axis of maximum moment of inertia by dissipation of internal mechanical energy. A special energy dissipator was developed for this spin-to-tumble transfer [7].

The satellites launched with the Juno 1 vehicle may be referred to as first generation payloads. In December 1954, the authors were assigned the task of developing an instrumentation payload for the Jupiter C multistage vehicle (Fig. 9.4). The objectives of the successful first firing of this Jupiter C (RS-27) were to flight test the upper solid propellant stage arrangement, the structure of the three stages, and a check on the function of a miniature Dovap transponder and the microlock. The payload was mounted on top of the inert fourth stage. This payload became the forerunner of the first satellite generation. Jet Propulsion Laboratory used the basic configuration of this payload for the Van Allen radiation experiment, called Explorer 1, when it was in orbit.

Correspondingly, the satellites developed for the Juno 2 carrier vehicle may be classified as second generation payloads. The configuration of both satellite types was established within the former Army Ballistic Missile Agency (ABMA). The first generation satellites had a cylindrical shape with 6-in. diameters and were approximately 36 in. long. The stainless steel shell was covered at its forward end by an aerodynamic blunt nose cone and was connected to the fourth stage by a fiber glass ring which served as a dipole antenna gap as thermal insulator against the last stage. For easy installation and accessibility,

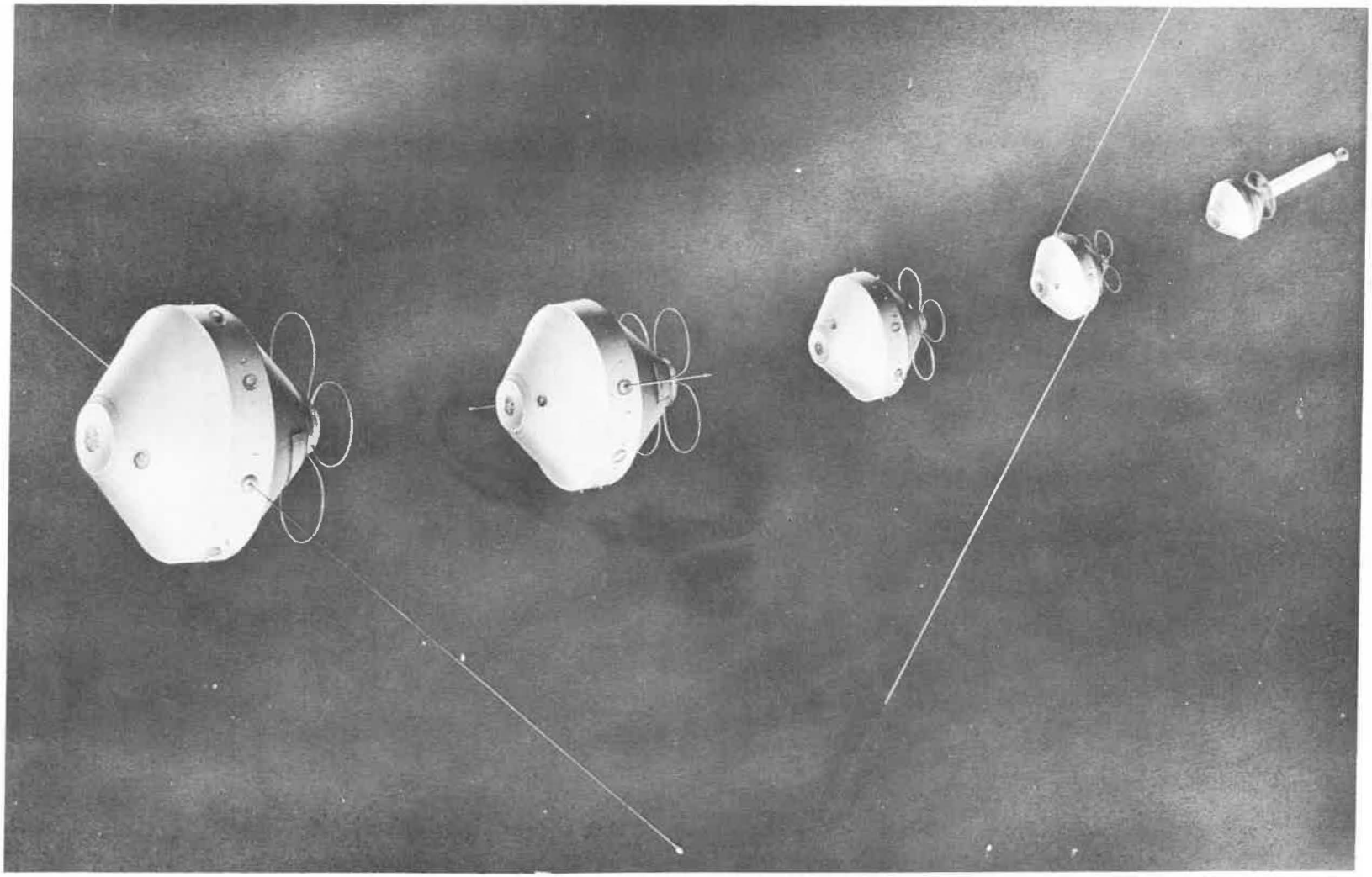

Fig. 9.3 Five f;ight phases of Explorer 8. (a) last stage separation; (b) first step spin reduction; (c) antennas begin to extend; (d) spin reduction continues; (e) orbiting satellite.

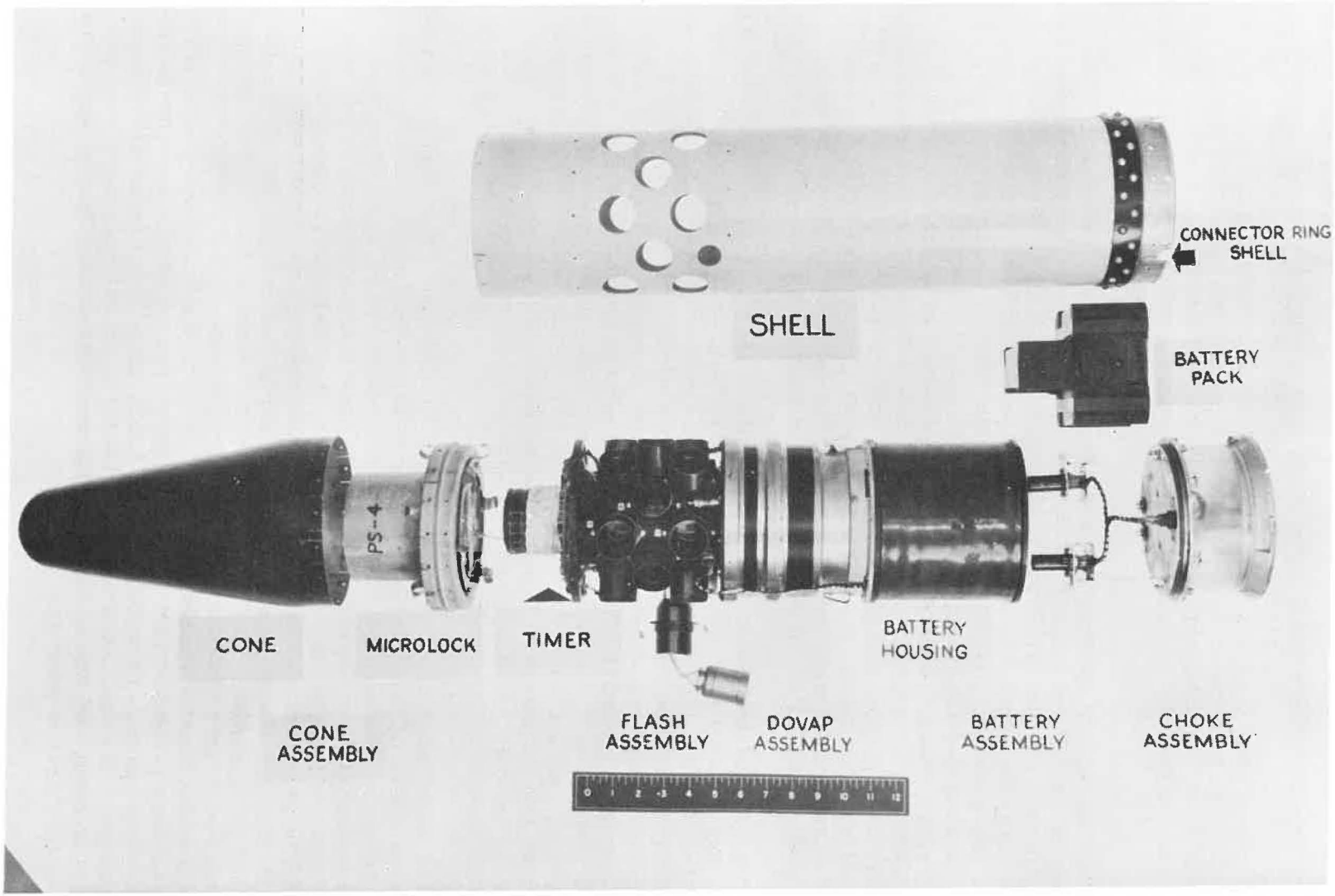

Fig. 9.4 Instrumentation payload for Jupiter C.

most of the instrumentation components were packaged so that they formed a column which exactly fitted the inside diameter of the satellite shell. The column design with its modules of 6-in. diameter and of varying thickness was also introduced into the second generation satellites, e.g., Explorer 7, 8, 11 and payload AM-19F (Figs. 9.5 and 9.6a, 9.6b). The instrument column was concentrically arranged about the spin axis (Fig. 9.7).

For the second generation satellites (excluding Explorer 11) the guiding design objective was to obtain an oblate mass distribution about the main axis of the spin-stabilized body (Fig. 9.8). The desired moment of inertia ratio was obtained by placing the relatively heavy batteries at the greatest possible distance from the spin axis (Fig. 9.7). In the following descriptions, Explorer 7 is used as a typical example. The external overall configuration was composed of a truncated double cone joined by a cylindrical center section. The connection between the centrally-placed instrument housing and the outer center ring was obtained by four spokes which sustained the centrifugal forces caused by spin, and also furnished support for the battery packs which were equally distributed at an equal radial distance from the spin axis.

The top and the lower truncated conical shell, made of polyester fiberglass, had to hold the center ring in position, and therewith the heavy batteries, during the impact of the thrust forces. The truncated cones were attached at the narrow opening to the rigid center column. At the wide opening, the cones were connected to profiled aluminum rings providing good transition of thrust through the center ring and sustaining the centrifugal load at the same time. The overall dimensions of the orbital carrier were 30 in. in diameter at the equator and approximately 30 in. in length. This method of packaging the instrumentation proved to be a noticeable advantage with respect to accessibility and exchangeability of components.

The required dynamic stability made it mandatory that separation of the empty shell of the last-stage rocket motor from the satellite occur after burnout. Because of tiny impulses generated by outgassing and afterburning, it was decided to set the separation approximately 2 min after burnout to avoid any collision with the shell or antenna wires. The timing was initiated by a timer in the third-stage rocket cluster. After 2 min, the delay timer caused the explosive charges in the separation device to ignite. It was necessary to assure instantaneous separation that would not produce an undue reaction to the satellite. A separation device was designed to this specification and was installed as a package, preloaded and sealed, between the satellite and the fourth-stage rocket motor. Material for the shell cones was either fiberglass or aluminum. The selection of the material greatly influenced the spin decay as a result of the generated eddy currents caused by the satellite's spin in the Earth's magnetic field.

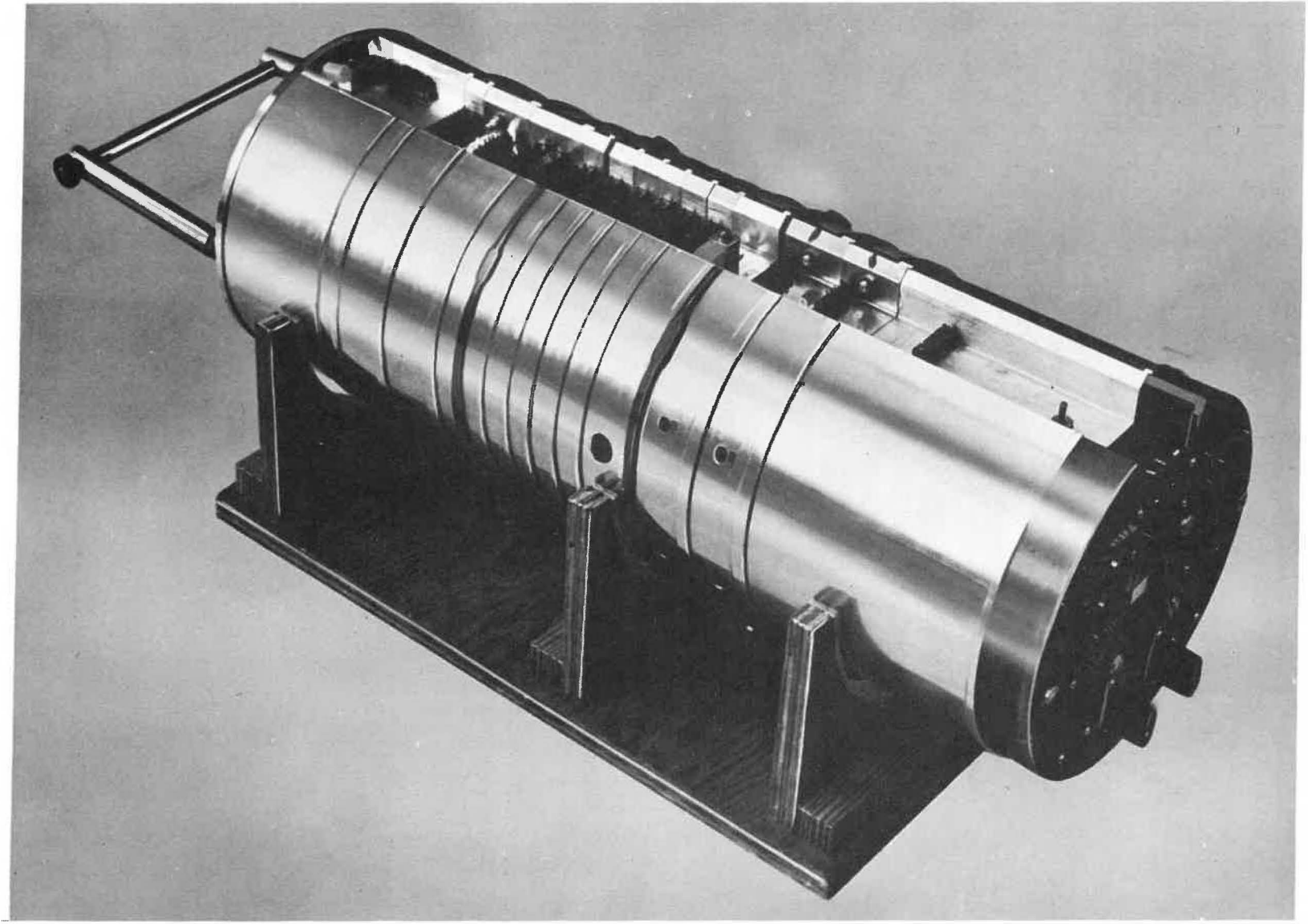

Fig. 9.5 Typical instrument column Explorer 11.

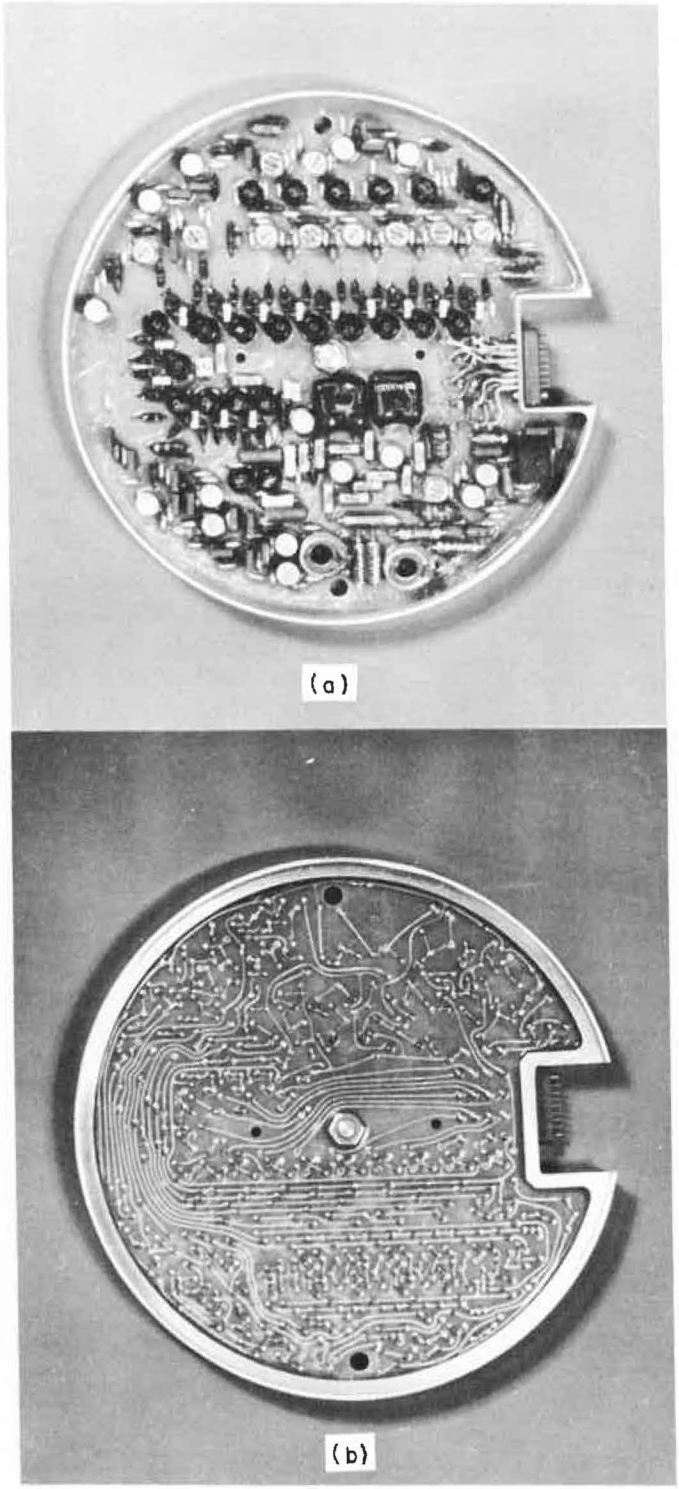

Fig. 9.6a Bottom view of typical module (telemetry of payload AM-19F).

Fig. 9.6b Top view of typical module (telemetry of payload AM-19F).

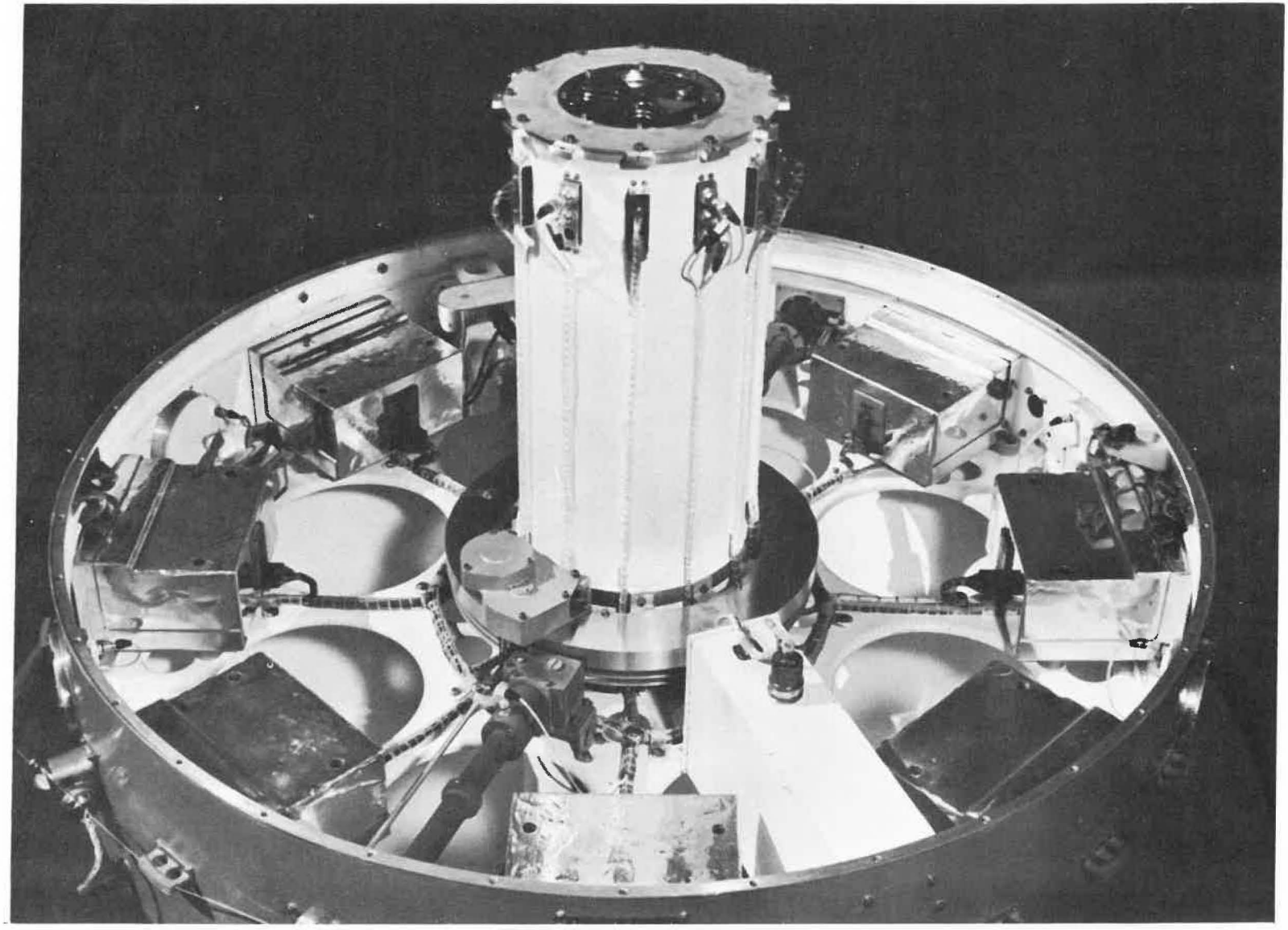

Fig. 9.7 Inside view of Explorer 8; top removed.

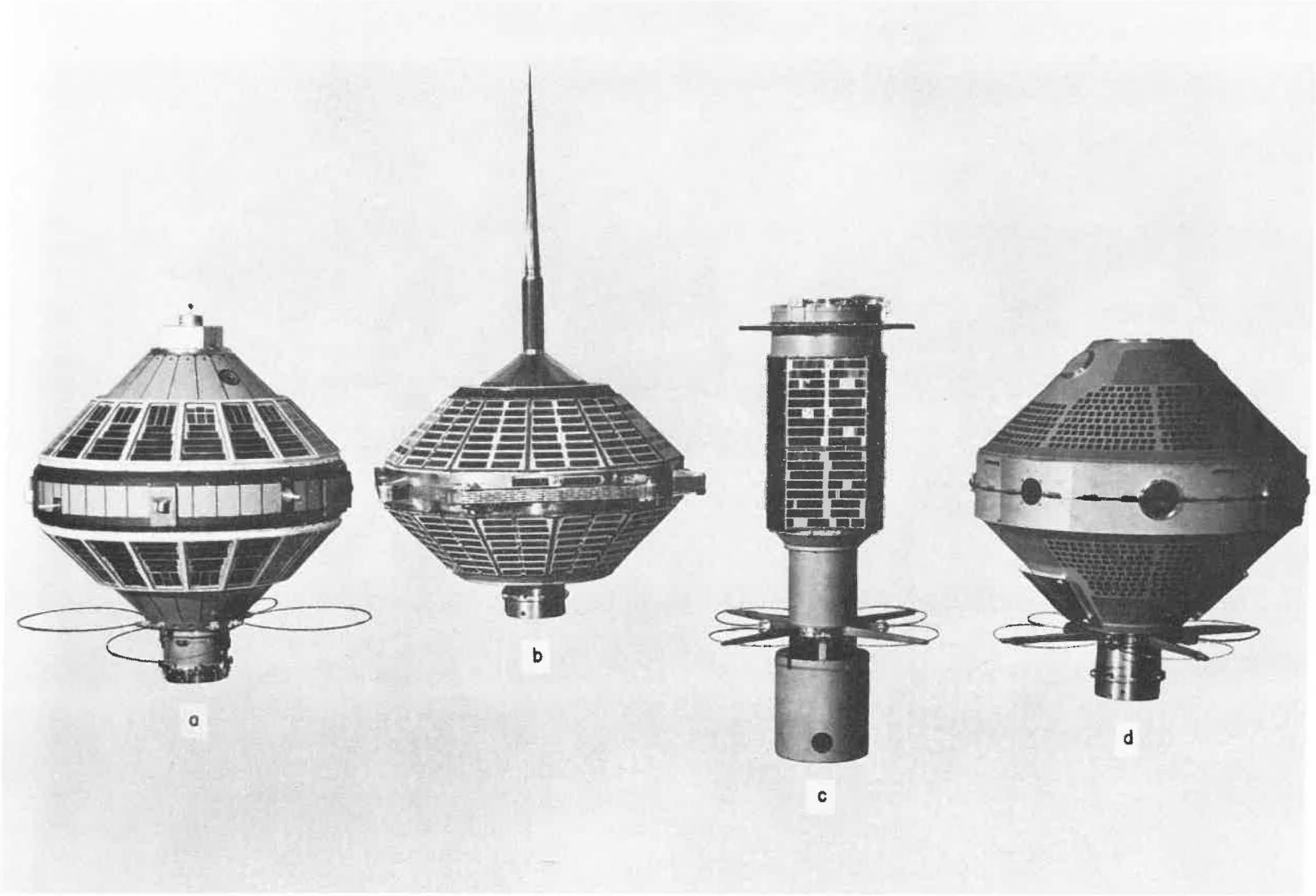

Fig. 9.8 Group of second generation satellites: (a) Explorer 7; (b) payload AM-19F; (c) Explorer 11; (d) Explorer 8.

The thermal calculations and testing had a decisive influence on the design by yielding satisfactory radiation and conductivity conditions for the satellite [8]. Sensing elements, instrumentation, and power supplies imposed temperature restrictions upon the orbiting satellite. Proper operation was guaranteed only when temperature fluctuations were held within prescribed ranges. Therefore, the instrumentation and batteries could not be exposed to temperatures lower than 0°C or higher than 60°C. The design of the satellites was influenced by thermal considerations. In Explorer 7, for instance, the thermal considerations affected the design in the following manner. The internal instruments and the batteries were insulated from the exterior hull of the carrier. The batteries were in thermal contact with the instrument column by four spokes. However, they were thermally detached from the satellite skin by Kel-F spacers, placed between the battery boxes and an aluminum ring composing a main structural element of the satellite shell at the equator.

With suitable emissivities on the outer skin surfaces, the desired thermal balance was achieved, indicating that acceptable internal average temperatures could be expected. Since the material of the shell was a thermal insulator, the outside of the shell had to be covered by a metal foil to reduce the temperature gradients along the skin and secure the necessary emissivities. The satellite configuration and the shell material made it necessary that the radiation exchange was directed to: (1) increase to the utmost the internal radiation exchange between the two truncated cones, and (2) diminish as much as possible undesirable energy exchange between the cones and the instrument column and batteries. To attain this controlled radiation exchange, the inside of the truncated cones was coated with titanium dioxide (TiO_2). All surfaces of the instrument column, battery supports, and battery boxes were covered with gold foil and were made of polished aluminum. A passive temperature control system was obtained in this way; the simplicity in this system meant greater reliability.

The various antenna systems developed for the different missions presented interesting mechanical design problems. To obtain efficient transmission for the 20-Mc transmitter of Explorer 7, an antenna of a radial wire length of approximately 12 ft was required. During the ascending, propelled flight phase, the space around the payload was limited by the protective shroud; therefore, an extended antenna system of desired dimensions was not applicable. Furthermore, the accelerations would not permit even the use of a lightweight rigid antenna of such size. Only an extensible antenna system was acceptable. The four antenna wires were stored by winding them into separate grooves on a common drum which was bearing-supported and motor-driven. The wires were unreeled simultaneously at nearly constant speed. The release started exactly when the separation of the last-stage shell took place.

For the indirect ionosphere measurements payload (AM-19F), a special circular and erectile loop antenna of 6 ft in diameter was the optimum solution for the transmission of three continuous frequencies (20, 40, and 41 Mc). The antenna consisted basically of four rigid arms and four flexible tape sections [9]. In the collapsed position, the arms, pivoted near the equator area, were tangentially arranged to the satellite body. The antenna was held in the collapsed position by means of restraining cords. At erection, the tape sections moved under velocity control so the final arrangement was a circular pattern, with the four arms swung out and locked in their outward positions.

9.3 The Satellite Instrumentation and Tracking Systems

The satellite program presented many new problems in the fields of instrumentation and tracking design and systems engineering. The instrumentation was determined by the specific mission; a basic problem was the design of circuits with very low power drains. This problem was solved with the use of switching transistors. By potting the printed circuit boards and mounting them together the problem of environments and physical space was solved.

The power output of the Juno 1 Explorer series satellites did not exceed 30 mw due primarily to the state of the art in transistors. The modulation used was determined by the ground receiving stations (microlock and minitrack). This was phase modulation of the tracking or low-power transmitter and amplitude modulation of the telemetry (communication) or high-power transmitter. The telemetry used low-frequency IRIG channels.

During the launchings of Explorers 1, 2, and 3, ABMA used for tracking a modified Dovap receiver with a sensitivity of approximately -128 dbm. The antenna system consisted of two stacks of four each Channel-6 TV antennas cut to 108 Mc. It had a gain of approximately 12 db and was motor driven in azimuth and elevation as well as in the plane of polarization.

During launch and the early weeks of orbiting, Doppler data were of primary interest. A digital print-out was made of the Doppler beat as well as recording it on tape with WWV time. Calculations were also made of the spin rate for the first few weeks. Of interest was the Faraday effect observed as the satellite passed over the horizons.

Experimentation was conducted during evening and night passes to see if the effect* of WWV transmissions reflected from ionized clouds which surrounded the satellite could be detected. This was never

---

* First noticed by Dr. J. D. Krauss of Ohio State University.

achieved, perhaps because not much time was devoted to the experiment. It must be pointed out that the indications Dr. Krauss observed coincided with the time the satellite passed overhead.

Recordings of the telemetry signals were also transcribed with reference to time at the ABMA station; however, the quality of the telemetry signal was only fair. There was no attempt to demodulate the telemetry signal at the station. The average length of a pass was between 6 and 7 min with a maximum signal strength of approximately minus 118 dbm.

The Juno 2 satellites presented a more difficult problem in system engineering than the Juno 1 series since the systems were much more complicated. Figure 9.9 is a typical system block diagram [10, 11, 12, 13].

For the second generation Explorers, several new ideas were used to aid both tracking and telemetry systems. A new method of phase modulation was developed to increase the reliability of the tracking signal (less phase jitter). A 1-w (nominal) AM telemetry transmitter operating at 20 Mc was developed; this was pushing the frontier of state of the art in transistors.

A novel crossed dipole antenna for this transmitter was extended after orbit was achieved. Very low frequency subcarrier oscillators were developed for Explorer 11 to allow information to be placed on a tape recorder which had a record playback ratio of 1 : 50; a whole orbit of information (100 min) was compressed into 2 min [14]. Other novel circuits used on this satellite were the command system (7-channel) and the pulse height-to-width converter for measuring very fast pulses [15]. See Figs. 9.6a and 9.6b for a typical instrumentation module. The use of the recorder multiplied the subcarrier oscillator frequencies by 50, thereby requiring wide bandwidth modulators and amplifiers. The S-45 satellite was unique among satellite systems because of the number of phase-correlated rf signals and the control of the basic oscillator frequency. The frequency was controlled by a crystal placed in a passive oven that used the heat of the Sun and the cold of space in the Earth's shadow for temperature regulation. Frequency stability was better than one part in 10^8 at 0.002° F temperature change per orbit [16].

For the launching of the Juno 2 Explorer series, phase-lock receivers were used for launch and orbital tracking. These receivers had a sensitivity of approximately -150 dbm. Antenna systems for 108 Mc consisted of colinear arrays with horizontal and vertical polarization with a gain of approximately 17 db and two quad-helix arrays with circular polarization and a gain of 20 db.

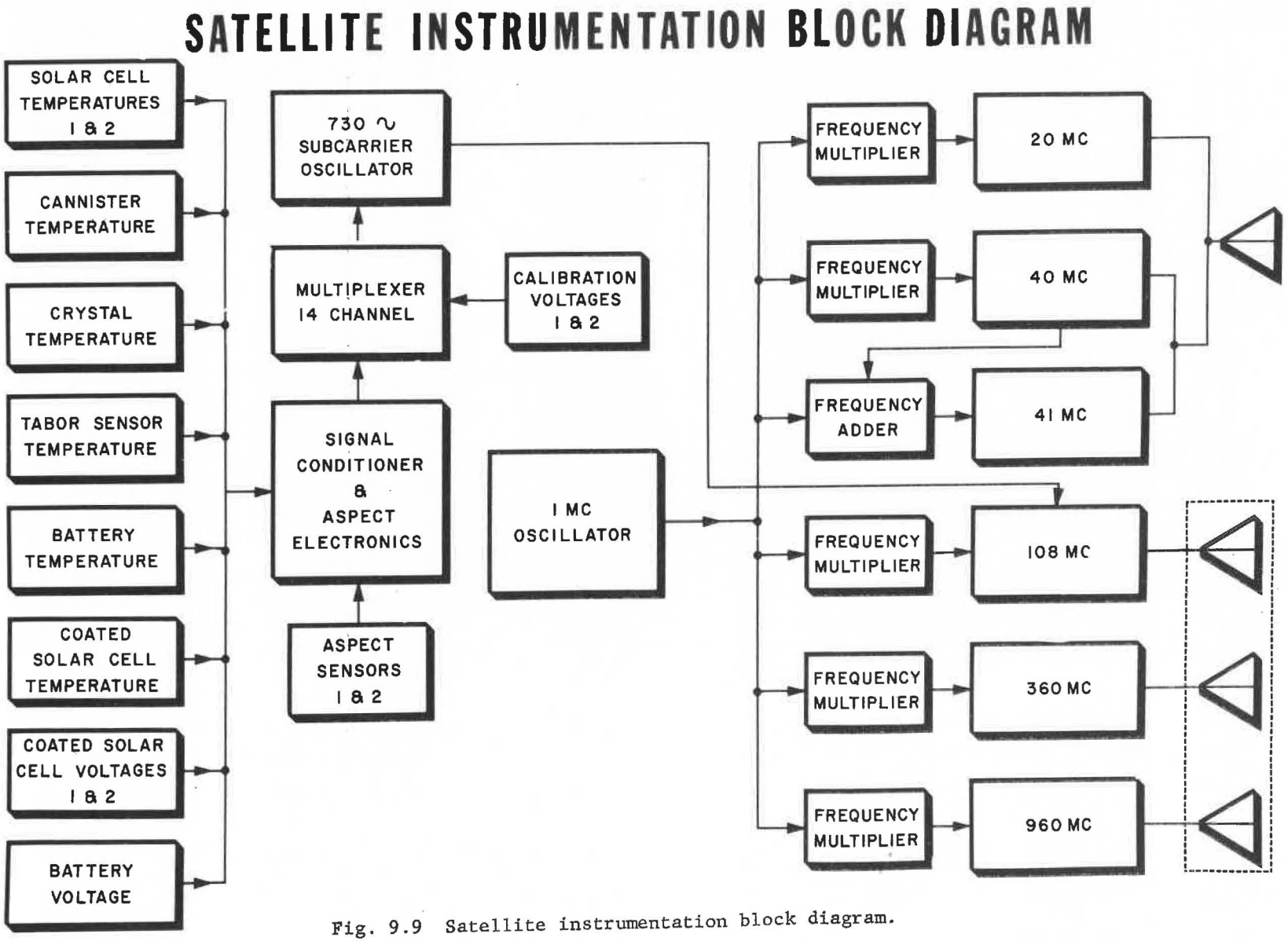

Fig. 9.9 Satellite instrumentation block diagram.

The antenna system used at 960 Mc included 14-ft and 10-ft parabolic dishes, each fed with a helix. The gain of the 14-ft dish was 30 db and the 10-ft dish was 27 db. The positioning and control system for the 108 Mc and 960 Mc antenna systems were modified SCR 584 radar control systems. The antennas have the capability of being positioned in aximuth and elevation.

Doppler data were recorded in digital and analog form; the Doppler beat was recorded on magnetic tape. Signal strength was recorded in analog form on a strip chart recorder and on magnetic tape. The composite telemetry signal was recorded on magnetic tape and it was also demodulated and recorded on a strip chart recorder. WWV time was recorded on magnetic tape and a strip chart recorder. A digital clock synchronized with WWV was recorded with the digital doppler print-out.

Modifications were made on the basic tracking system to optimize the system depending on satellite characteristics. In the case of the Pioneer 3 a converter was designed for 960 Mc which required multiplying the voltage control oscillator by 18. A Doppler count modification kit was also designed which converted the Doppler frequency suitable for use with an electronic counter while still maintaining the required accuracy.

A parametric amplifier was used to track Pioneer 4 to approximately 168,000 miles. It is believed the system held lock to approximately minus 153 dbm.

Explorer 7 was equipped with two transmitters, one at 20 Mc and amplitude modulated; the other transmitter was at 108 mc and was phase modulated. A Collins R-390 receiver was used to receive the 20 Mc signal with a low noise preamplifier added to the rf stage. A Yagi antenna with 6db gain, capable of being positioned in azimuth only, was used for receiving the 20 Mc signal. The 20 Mc receiver had a sensitivity of approximately minus 125 dbm. The receiver for 108 Mc and the recording system were described in previous paragraphs.

Explorers 8 and 11 used wide-band telemetry systems. The phase lock receivers had a predetection bandwith of 3 kc; therefore, it was necessary to modify the 455-kc amplifier as well as the phase detector to pass the information. The bandwidth was modified to 50 kc.

The AM-19F and AM-19G satellites (S-45) presented a problem in ground receiving system design. These satellites were designed to transmit low power, phase coherent signals at frequencies of 20, 40, 41, 108, 360, and 960 Mc. These frequencies were chosen for determining the propagation characteristics of the ionosphere by measuring the relative

phase delay of signals transmitted through the ionosphere from a satellite by the differential Doppler technique and Faraday rotation.

A receiving system capable of accurately measuring the phase difference between any two pairs of the six frequencies and maintaining phase coherence with the received signal was needed. Such a system was designed, based on the phase lock principle. The Doppler shift was tracked by the locked loop and normalized in all receivers so its effect does not appear in the phase difference information channel. Drift in the transmitter oscillator frequency as well as drift in the local oscillator frequencies are also cancelled in the ground system. The sensitivity of the system was approximately -150 dbm. Due to such a high sensitivity, the system required very careful attention in filtering and shielding because the local and reference oscillators are multiples of 1 Mc, and the harmonic and mixer products generated in the system may fall on or near the signal frequency. Therefore, careful shielding and filtering were employed to avoid desensitization of the system and false locking.

Several unusual problems were encountered in the design of antennas for the satellite payloads orbited by the Jupiter C., Juno 1, and Juno 2 vehicles. Weight and space requirements necessitated the use of electrically small antennas in many cases, and the resulting problems of bandwidth and efficiency, together with restrictions on solar cell shadowing, continued to produce some rather novel antenna designs. The use of spin stabilization on these satellites also imposed certain pattern requirements to avoid modulation of transmissions by the spinning motion of the satellite. Probably the most elaborate and unusual antenna system used in the satellite program was that employed by the AM-19F and AM-19G ionosphere beacons (S-45). The satellites were designed to transmit six continuous frequencies over a wide frequency range with linear polarization, constant amplitude, wide angular coverage, and high efficiency. The two antenna assemblies used to transmit these frequencies consisted of a multifrequency loop and a composite arrangement of linear elements, all of which were packaged inside the small space permitted by the Juno 2 shroud. Figure 9.10 shows several satellite antenna configurations [17].

9.4 The Power Supply System, Electrical Networks, and Timing Devices Of the Satellites

To make various satellite configurations operational in space, electrical power is needed. Electrical power has to serve the communications and tracking systems, the measuring instruments, timers for switching functions, separation devices, and antenna release mechanisms.

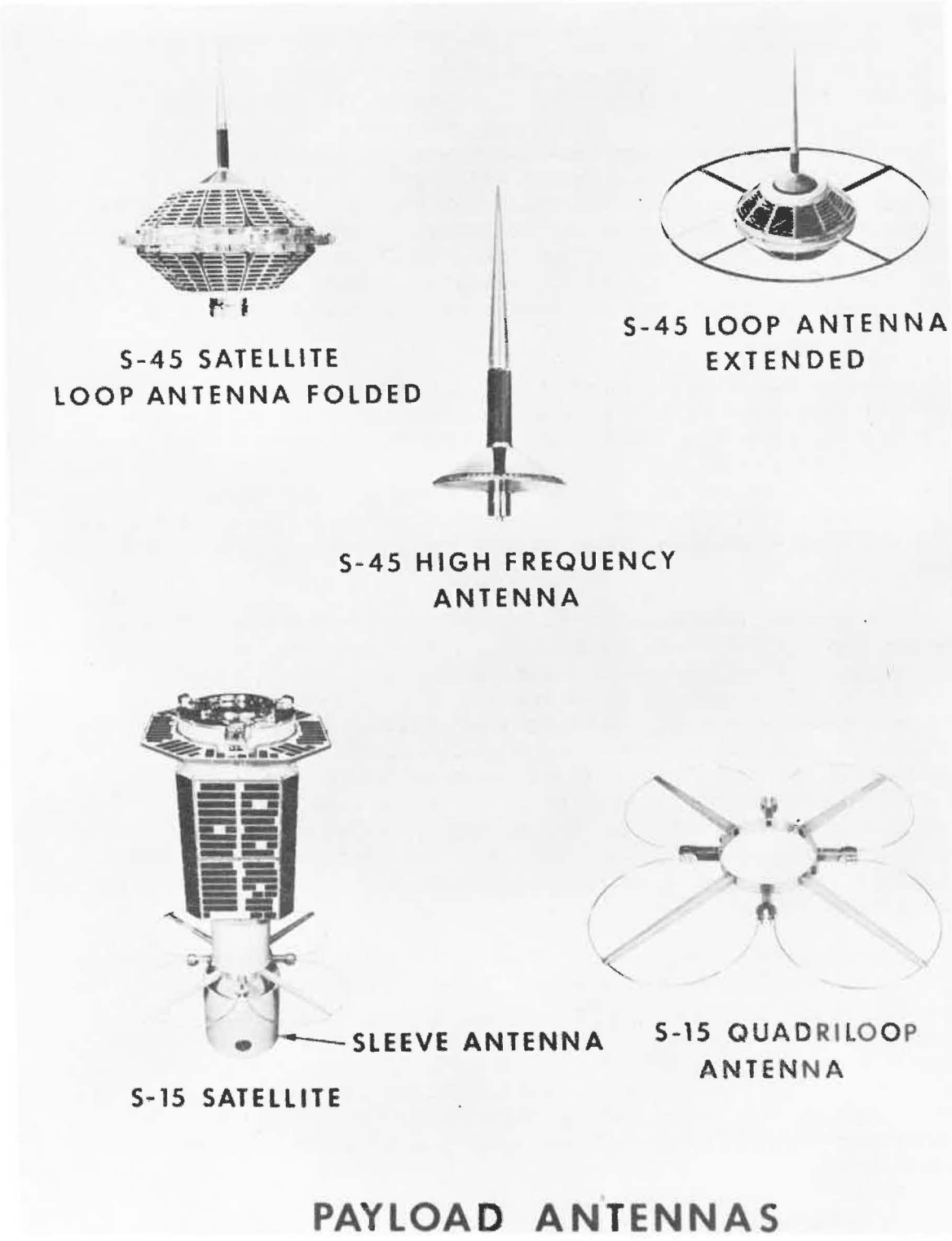

Fig. 9.10 Satellite antenna configurations.

Dependent on the desired operational lifetime of an experiment, the power source has to be selected. Mercury batteries can operate experiments for a lifetime of up to 8 weeks. If the expected lifetime is longer, other means of electrical power supplies must be chosen. Solar power conversion was used in several satellite systems and excellent results were achieved. Solar cells in conjunction with nickel cadmium batteries for storage of electrical energy were the power supply system in many applications. Table 9.3 shows the power sources for different satellites, the overall power consumption, and designed life time. To describe a typical design approach of a solar cell power supply system, the S-46 satellite design approach will be shown [18].

Within given weight limitations and configuration requirements, several approaches had to be studied. Various configurations were considered, including three- and four-finned cylinders. Preliminary calculations showed that the requirements of a light weight, constant-power output system could be met by placing an equal group of cells on each side of a rectangular body. This application required that the rectangular body be placed around the cylindrical instrument housing.

To prevent reverse current flow between the cells illuminated by the Sun and the cells on the dark side, diodes had to be inserted in series with each group of solar cells. The loss of about 0.7 v per diode had to be considered for the overall voltage output. Several power and voltage outputs were required for transmitter, subcarrier oscillator, and instrumentation totaling about 1300 mw. The operational voltages were established considering nickel cadmium batteries continuously connected to the solar cell power system during charge and discharge cycle. The maximum charging voltage was limited by zener diodes and a certain cell deterioration was assumed during discharge. This gave a voltage variation of $\pm$ 11.5 per cent about the nominal value.

Calculations indicated an orbit period of about 10 hr with about 2 hr of Earth shadow for the satellite as a maximum. There would be periods of 100 per cent sunlight orbit, giving a maximum solar cell temperature of about 80°C. Subsequent studies also indicated more than 2 hr shadow time and required a careful selected firing time to stay within the 2 hr of Earth shadow time for adequate design of the power supply. The solar cell arrangement was based on the maximum temperature of 80°C, and cell losses had to be considered for this temperature.

To obtain extremely long cycle life (over 5000 cycles) from sealed nickel cadmium batteries, it was necessary to limit the discharge to about 10 per cent of total battery capacity. Eight

Table 9.3 Satellite Power Sources

Satellite	Power Source	Power Consumption (milliwatts)	Designed Lifetime
Explorer 7	Solar cells paralleled with nickel cadmium batteries (6 different voltages)	2642	Transmitter cutoff by timer after 1 year.
	Mercury batteries (3 different voltages)	94	
S-46	Solar cells paralleled with nickel cadmium batteries (3 different voltages)	1328	Transmitter cutoff by timer after 1 year.
Explorer 8 (S-30)	Mercury batteries (33 different voltages)	946 continuous 3157 intermittent	Approximately 1.5 months.
S-45 (Payloads AM 19F & 19G)	Solar cells paralleled with nickel cadmium batteries (1 voltage	2639	Transmitter cutoff by timer after 1 year.
Explorer 9 (S-15)	Solar Cells paralleled with nickel cadmium batteries (4 different voltages)	1616	Expected life of satellite was 1 year; transmitter can be turned off by ground command. Last minute change of orbit revised power source life expectancy to 4 months, since the satellite will be exposed to radiation belt with no solar cell protection.

hundred and sixty orbits for 1 yr of operation of S-46 were expected with more than 50 percent of the orbits in full sunlight. This meant not more than 400 to 450 cycles for the batteries.

At very low charging rates, about 150 per cent of the ampere-hours delivered on discharge must be returned to the battery during charge. The average charging current to return the battery to the fully charged condition is given by

$$I_c = \frac{I_l \times T_l}{T_c \times \eta_{ah}}$$

where

I_c = Average battery charging current required from solar cells

I_l = Average electronic load current

T_l = Maximum time per orbit battery is under load

T_c = Minimum time per orbit battery is receiving charge

η_{ah} = Ratio of ampere-hours delivered from battery under load to ampere-hours required to return battery to fully charged condition

The incident solar radiation outside the Earth's atmosphere is approximately 140 mw/cm^2. This value can vary by plus or minus 3.4 per cent as the Earth moves from perihelion to aphelion. The spectral distribution of the solar radiation approximates that of a 5900°K black body. A plot of the distribution of this radiation is shown in Fig. 9.11 together with the spectral response plot of a silicon solar cell. It shows that the solar cell responds to the wave lengths between approximately 0.4 and 1.2 μ. Integration of the solar energy distribution curve shows that this wave length band contains approximately 55 per cent of the total solar energy available. Other factors, such as reflection losses, internal resistance losses, and junction property restrictions, limit the maximum theoretical conversion efficiency of silicon solar cells. In connecting solar cells in series, mismatch in voltage-current characteristics and connection resistance reduces the over-all efficiency of groups of cells even further. For the predicted cell temperature of 80°C, the efficiency has to be further reduced. It is 71 per cent of its value at 30°C.

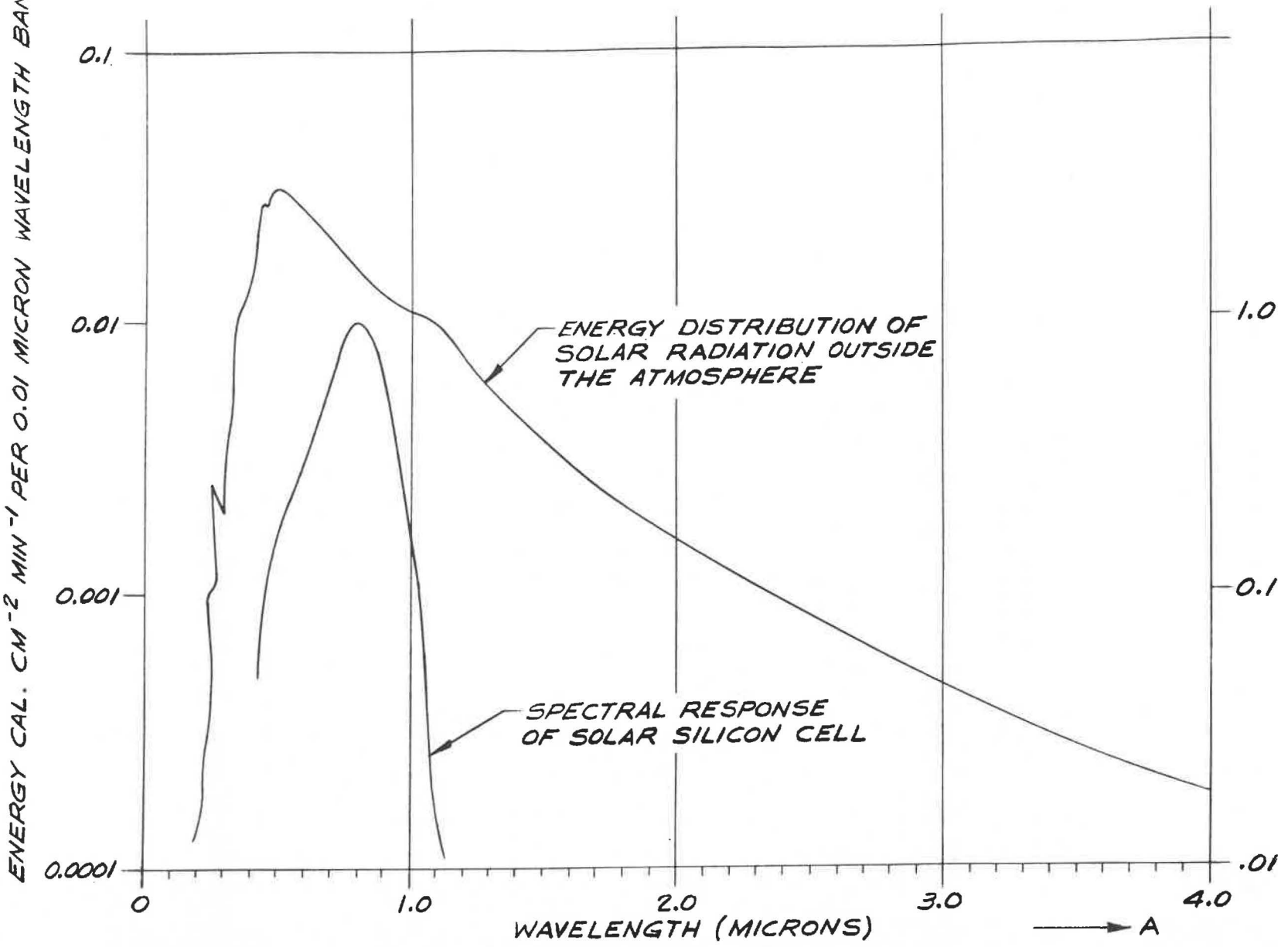

Fig. 9.11 Spectral distribution of solar energy and spectral response of solar cells.

The required power output of the solar cells is given by

$$P_o = I_o V_o$$

where P_o = power output of solar cells in milliwatts

I_o = sum of electronic load current and battery charging current in milliamperes

V_o = sum of average system voltage and voltage drop across blocking diode

The number of series connected cells required for each voltage was determined by dividing V_o by the optimum cell voltage at the maximum expected temperature.

With the solar cell surface perpendicular to the Sun, the total solar cell area needed to produce the required power is given by

$$A = \frac{P_o}{\eta K}$$

where

A = active solar cell area in sq cm

η = group solar cell efficiency at design temperature

K = solar constant in mw per sq cm

From this equation, the number and type of cells for each power supply was determined.

To completely analyze a solar cell system layout for a nonoriented satellite, it is necessary to evaluate the design for the effects of variation in light incidence on the power output that results from:

1. Aspect of axes with respect to the Sun.
2. Tumble.
3. Rotation or spin.
4. Shadow from protruding parts.

In the case of S-46, the satellite was a cylindrical body of the diameter of the last-stage rocket. A rectangular box was required to provide adequate area to mount solar cells for the mission. After the battery capacity was established, the solar cell groups were designed. The layout provided for proper distribution on each of the six sides of the structure. Special care had to be taken in cell

placement on top and bottom plates to avoid undue shadowing of any cell group by the instrument housing or the fourth-stage rocket protruding through the solar cell box assembly.

The general equation for analyzing the effect of satellite rotational position on the solar cell system output can be based on the assumption that the power generated varies directly with the cosine of the angle between a line normal to the cell surface and the incident light vector. The curves shown in Fig. 9.12 relate the power output of a typical silicon solar cell to the angle of incidence of light for a fixed load. Although the curve for optimum power would follow closely the true cosine curve, the fixed load curve must be used for this type of analysis. This is not reflected in the general equation to be derived. Corrections for deviations from the true cosine function are to be made when the problem is fed into the computer.

To utilize an analog computer for plotting all possible satellite positions which may occur, some equations can be established using Fig. 9.13 for the geometric relations.

For side 1

$$\cos\gamma_1 = (\cos\phi \quad \sin\beta \cos\theta + \sin\phi \sin\theta)$$

For side 2

$$\cos\gamma_2 - \cos\phi \sin\beta \ (\theta - 90^o) + \sin\phi \sin \ (\theta - 90^o)$$

For side 3

$$\cos\gamma_3 = \cos\beta \cos\phi$$

The results of this analog computer simulation of the problem are shown in Figs. 9.14 and 9.15. The average relative power per cycle of tumble rotation was plotted against the spin rotation angle θ to demonstrate the effect of spin spuerimposed on tumble for fixed values of ϕ (the angle of the Sun with respect to the plane of tumble rotation). By integrating the curves for $\phi = 0$ deg and $\phi = 90$ deg, the minimum and maximum average relative power for the system was obtained for simultaneous spin and tumble.

One of the major problems in establishing a functional satellite is the integration of various assemblies, sensors, and power supplies into a complete functional system. This requires the cooperation of the electronic, structural, electrical and thermal designers.

The electrical network combines all electrical components into the desired operational system as defined by the mission. Careful

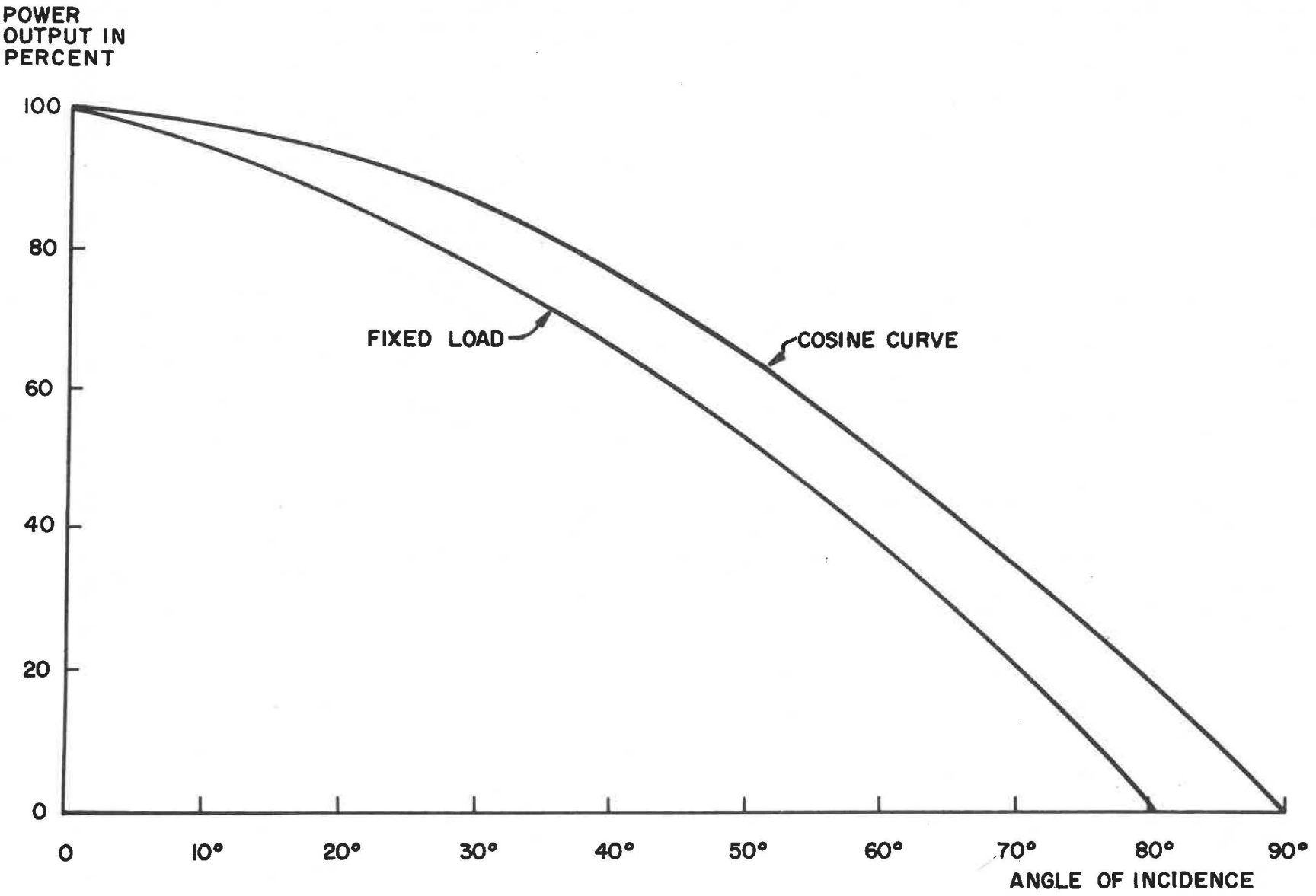

Fig. 9.12 Silicon solar cell output versus light incidence.

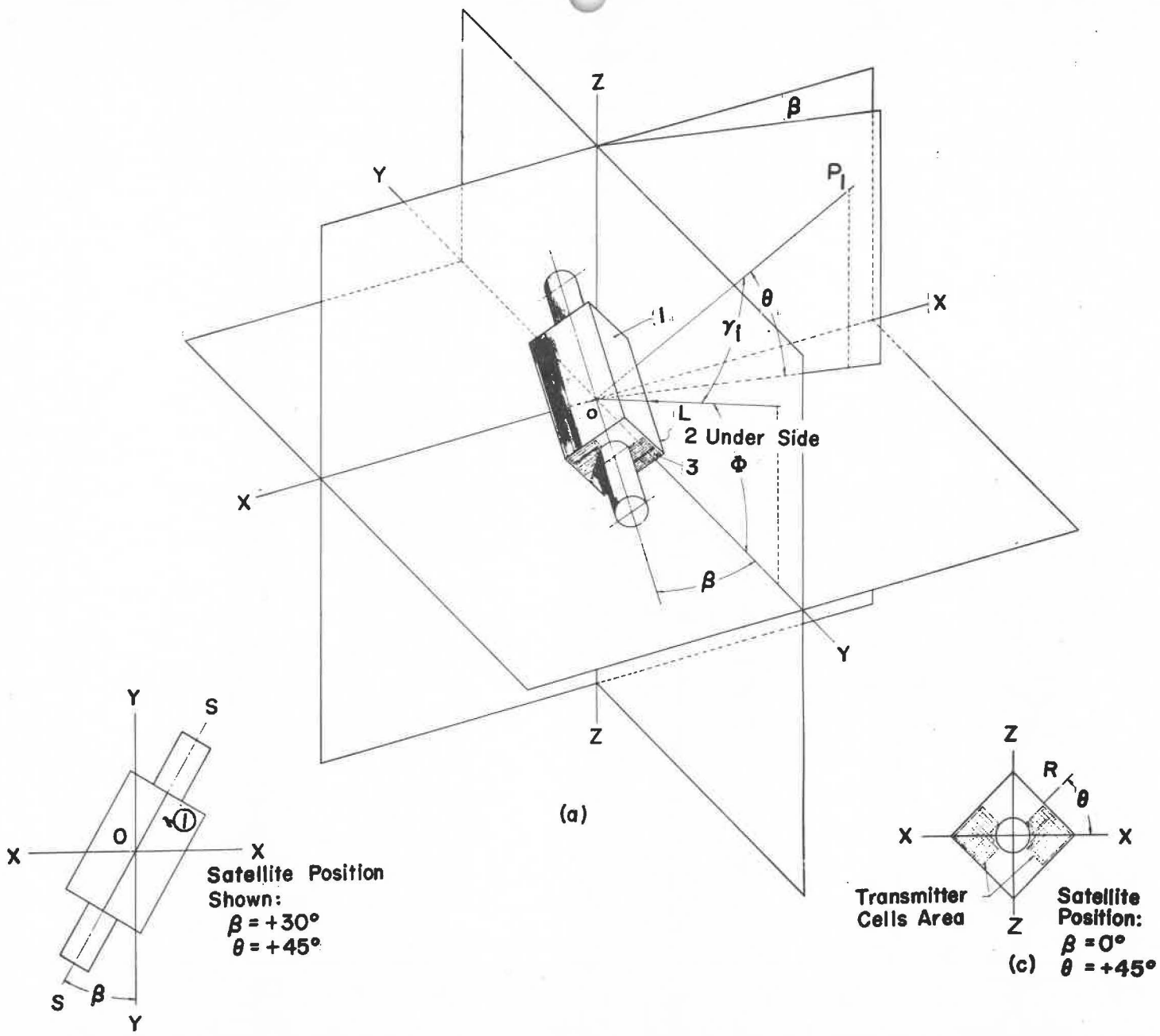

Fig. 9.13 Arbitrary space position of satellite S-46 for establishing satellite position equations.

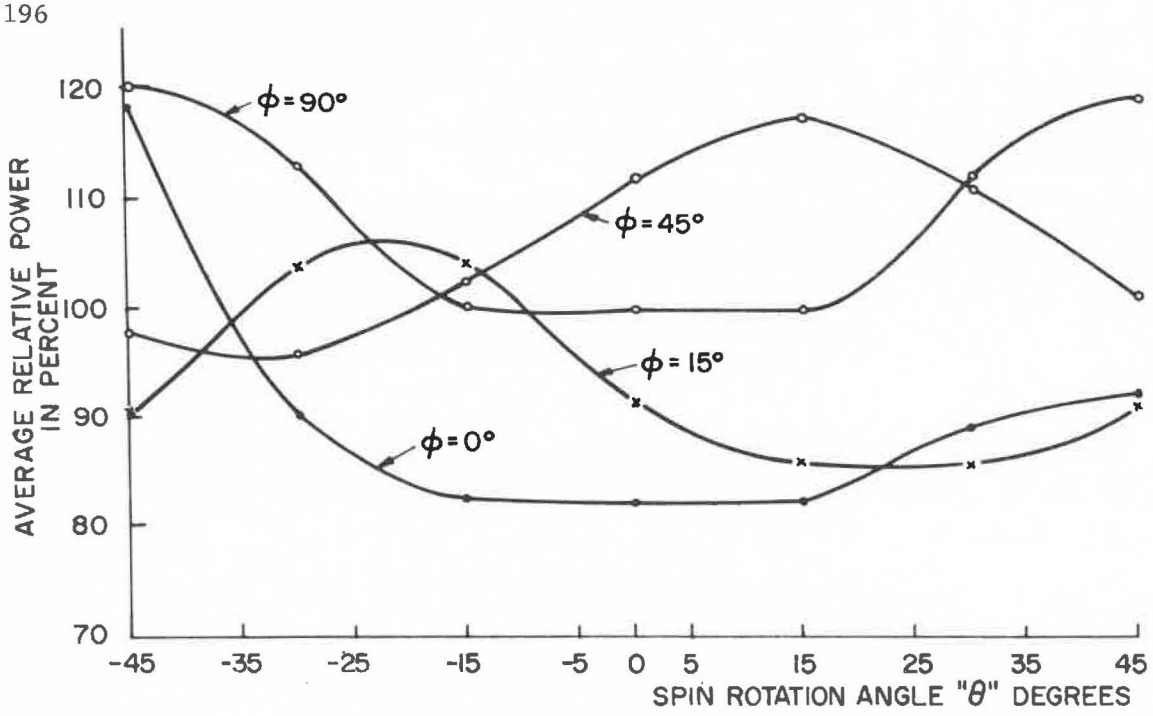

Fig. 9.14 Relative average power per tumble cycle as a function of spin rotation at 0^{o}, 15^{o}, 45^{o}, and 90^{o}.

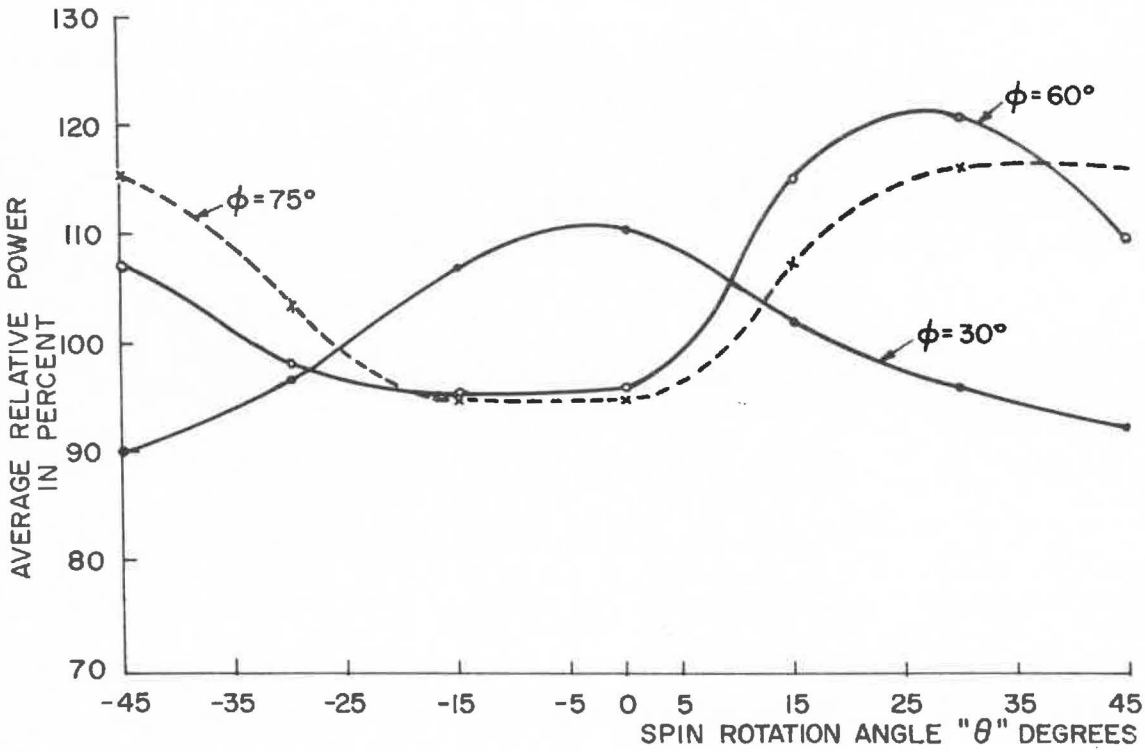

Fig. 9.15 Relative average power per tumble cycle as a function of spin rotation at 30^{o}, 60^{o}, and 75^{o}.

planning is necessary to assure functional compatibility of the entire system. Power requirements define the power sources. To save weight, these sources must be shared by several consumers. Still, interference-free operation has to be achieved. The systems design has to be approached with a great amount of flexibility to allow modification of the different subassemblies, if required by the advancement of design or development. The electrical system is designed by utilizing a modular construction. A distribution center will provide the flexibility for changes and serve as a central point for power distribution, timing, and sequencing functions. The various modules should be connected to the distributor by cables and connectors to maintain ease of module exchange.

The S-46 satellite again can serve as a typical example for this design philosophy as utilized in the different satellite configurations launched under our assigned program.

Checkout and preflight monitoring is an important part of electrical systems design. An assembled satellite has limited access for operational checking. This access is even less after mating with the overall space carrier vehicle. The status has to be monitored during preflight and actual launch countdown to assure satisfactory systems performance prior to launch. Timing devices, a part of most satellite electrical systems, were used to sequence proper payload separation from the last stage, unreel antennas, blow off shrouds, etc. The RC timers were part of the network and could execute several functions in sequence. For satellites powered by solar cell systems, another long duration timer was developed to cut off the entire system at a desired preset time. To avoid saturating a frequency band with useless radio signals, it was necessary to include such a timer to shut off the transmitter on Explorer 7 after 1 yr of operation. Otherwise, the transmitter could possibly operate as long as the solar cell power system continued to function.

A 1-yr electronic timer was deyeloped by Bulova for this special purpose, operating on its own power source. The timer had no escapement; it operated on a transistor switch-operated tuning fork mechanism, with an accuracy of better than 0.1 per cent.

9.5 Environmental and Functional Testing of the Satellites

A vital prerequisite for the successful performance of the satellites was comprehensive and rigorous testing with respect to functions and environmental conditions. The test program gave optimum simulation of all expected environmental conditions to be encountered by the satellites during the ascending phase of its trajectory and while in orbit. In particular, exhaustive functional tests were performed with individual component systems.

The applied test procedure provided tests with prototype models, and also flight acceptance tests with the actual flight satellite. The prototype models completely resembled the satellite to be launched. Accordingly, separate test specifications were prepared for prototype acceptance containing well-founded safety factors. The satellites to be launched were subjected to basically the same series of tests under substantially less rigorous conditions. The main intent of these tests was to investigate the satellites after final assembly in order to determine the extent of human error.

Several prototypes were manufactured for mechanical, electrical, and other tests, which were often run in parallel. Findings of the prototype testing were evaluated and, where necessary, led to corresponding modifications which were considered before the manufacture of the flight satellite.

The Juno 1 and Juno 2 rocket systems, with the cluster rotating up to 750 rpm and 450 rpm, respectively, imposed stringent requirements on balancing the satellites. For example, the radial distance of the center of gravity from the spin axis of the 92.3 lb Explorer 7 satellite was to be smaller than 0.005 in. The dynamic tests were performed with a highly sensitive special balancing apparatus. Because the design is rotationally symmetric, the balancing weights which had to be added resulted in only a small weight penalty.

Another essential phase of the test program represented the testing of the effects of static and dynamic accelerations produced by spin, thrust, initial shock, and vibrations. The satellites were spun on a mechanism at a rate of 600 rpm for at least 5 min. Functional operation of the payload instrumentation was monitored during the spin period. This was to prove: (1) the structural adequacy of the satellites; and (2) the perfect functioning of instrumentation and the complete power supply under spin.

The complete satellite assemblies were mounted on a centrifuge and subjected to accelerations caused by first stage thrust and the cluster rockets. Instrumentation and power supply were checked before and after a 3-min exposure to acceleration. By spinning the satellites on the centrifuge, centrifugal acceleration was superimposed on thrust acceleration.

To simulate the acceleration conditions during propelled flight, the entire payload of the Juno 1 missions was spun on the revolving centrifuge. It was necessary to abstain from exposing the entire satellite of Juno 2 missions because of unacceptable gyroscopic torques. Therefore only the instrument column of these satellites was subjected to the superimposed accelerations. The initial shock resulting from the three solid propellant rocket stages was checked by a linear accelerator. Thirty shock exposures to about 25g and 10 msec duration

were imparted to the instrument column. The test apparatus used was a newly developed linear accelerator, working cyclically on a pneumatic principle. The behavior of the satellite was tested, with regard to the structure and the operation of the instrumentation under the impact of rocket vibrations, by vibrating the satellite in three directions about three mutually perpendicular axes, one of which was the spin axis.

The orbital environments were simulated with respect to vacuum and temperature, after the satellites were exposed to launch environments. For obvious reasons, the condition of weightlessness could not be simulated. The instrumentation and power supply (except solar cells) worked in near vacuum over the anticipated range of temperature. The thermal characteristics of the satellite were determined to enable prediction of orbital temperature ranges by analysis. Liquid nitrogen and a special electric heating blanket were used in a vacuum chamber to cool the satellites to a low temperature and to heat it up by a heat-step which could be directed to all or part of the satellite's surface. In this way, internal conductive and radiative coefficients of the satellite were determined and evaluated in order to calculate, in connection with the surface emissivity ratios, the temperatures for certain orbital data.

The satellite's capability to operate over longer periods in space was investigated by subjecting the satellite to a vacuum of 5×10^{-5}mm of mercury at instrumentation temperatures between 5° and 55° C $\pm$ 5° C, respectively, for 2 weeks. For 1 week, each of the extreme temperatures was applied; they represent the extremes of the permissible temperature range. During this vacuum-temperature "soak" test, the functioning of all the experiments (except the solar cells) was continuously monitored.

Spin decay was investigated by means of a specially developed apparatus for generation of a highly homogeneous magnetic field. After completion of satellite assembly, electrical tests were performed to verify the circuitry and the capability of the power supply to operate the various electronic components. Operational tests were run to certify the antenna patterns, field intensity and compatibility of transmitters with the microlock stations.

Typical of the way functional testing was executed were the following two tests performed with component systems. Both elements had to operate perfectly, the separation device which was applied in all cases when the empty shell of the fourth-stage motor was disconnected from the satellite, and the 20-Mc antenna release mechanism as flown with Explorer 7. The malfunction of either one of these components during the actual flight would have resulted in a total failure of the mission.

The separation device, after all its parts had been checked rigorously, was tested under closely simulated flight conditions so that the dynamic behavior of the complete system, consisting of satellite and empty shell of last-stage motor, could be observed. A satellite mock-up of true mass distribution was suspended at its center of gravity, with low friction, by a cord. In this way, the six degrees of motion freedom were approximately simulated. A rocket dummy, also representing an actual mass distribution, was attached to the dummy satellite by the separation device to be tested. After the system was spun up to the cluster rpm of 450 and nutation was artifically imparted, the separation mechanism was actuated. It was found that the applied mechanical scheme was sound and reliable. The separation was instantaneous and without noticeable reaction to the satellite body.

The extensible 20 Mc antenna system of Explorer 7 was also tested under a close simulation of possible flight conditions. The test program was based on full-scale operation of the antenna system in a large vacuum chamber, a 41-ft diameter sphere, at 1 to 2 mm of mercury. The satellite was suspended as it was for the separation test. The motion of the wires and the satellite was observed. Nutation of a varying amount was generated by the dropping of weights onto the simulated satellite. The operation of the mechanical system to full wire extension with and without nutation, the damping capability of the extended wires, the wire release velocity, and the spin decrease caused by inertia increase by change of mass distribution, were studied and checked. The antenna release system was accepted for flight after a considerable number of operations had been performed satisfactorily in every respect.

The test program outlined above was based on the philosophy that high reliability is achieved not only by suitable design but also by the quality of the tests.

REFERENCES

1. von Braun, Wernher, A Minimum Satellite Vehicle Based on Components Available from Missile Development of Army Ordnance Corps, Guided Missile Development Division Ordnance Missile Laboratories, (Redstone Arsenal), Huntsville, Alabama, September 15, 1954.

2. Haeussermann, Walter, Spatial Attitude Control of a Spinning Rocket Cluster, ARS Journal, 20: 56-58 (January 1959).

3. Explorer 1, prepared by Jet Propulsion Laboratory, Astronautics 3: 20 (April 1958).

4. Boehm, Josef, Considerations to the Development of Explorer 7 Satellite, IRE Transactions on Military Electronics, MIL-4: 86-92 (April-July 1960).

5. Pfaff, Helmuth, Combined Antenna - Release and Despin - System (Second Phase) for Payload 19D (S-30), Rept. MM-M-G&C-2-60, NASA-Marshall Space Flight Center, Huntsville, Alabama, August 10, 1960.

6. Counter, Duane N., Spin Reduction for Low Probe Satellite S-30 (19 D), Rept. MNN-M-G&C-5-60, NASA-Marshall Space Flight Center, Huntsville, Alabama, September 12, 1960.

7. Kuebler, M. E., Tumble Transfer of Satellite S-15 (Explorer 11), Rept. MTP-G&C-61-30, NASA-Marshall Space Flight Center, Huntsville, Alabama, July 10, 1961

8. Heller, Gerhard, Problems Concerning the Thermal Design of Explorer Satellites, Rept. No. DV-TM-11-60, Army Ballistic Missile Agency, Huntsville, Alabama, May 17, 1960.

9. Wagner, Hermann R., Payload S-45 Development Report (Mechanical), Memo M-G&C-MM, NASA-Marshall Space Flight Center, Huntsville, Alabama, July 25, 1961

10. Instrumentation Description and Checkout Procedures for the Gamma Ray Satellite, S-15, Rept. MTP-M-G&C-61-16, NASA-Marshall Space Flight Center, Huntsville, Alabama, March 17, 1961.

11. Checkout Procedure for Missile 16-S Payload, ABMA Report, G&C Laboratory, Huntsville, Alabama, February 11, 1959.

12. S-46 Satellite Instrumentation, ABMA Report, G&C Laboratory, Huntsville, Alabama, February 9, 1960.

REFERENCES (Cont'd)

13. Instrumentation for the Ionosphere Beacon Satellite S-45, Rept. MTP-M-G&C-61-4, NASA-Marshall Space Flight Center, Huntsville, Alabama, February 8, 1961.

14. King, Olin andFrank, Emens, Data Transmission System for the Gamma Ray Astronomy Satellite, Proceedings of National Telemetering Conference, Chicago, Illinois, Paper 4-37, May 1961.

15. Malone, Lee, Radio Command System for the Gamma Ray Satellite Experiment S-15, Rept. MNN-M-G&C-2-60, NASA-Marshall Space Flight Center, Huntsville, Alabama, July 20, 1960.

16. Fisher, Alan J., Final Engineering Report Satellite S-45 Ionosphere Beacon Transmitter, Rept. MTP-M-G&C-61-16, NASA-Marshall Space Flight Center, Huntsville, Alabama, March 10, 1961.

17. Harper, J. W., and Swindall, P. M., Final Engineering Report on Satellite S-45 Antenna Systems, Rept. MTP-G&C-I-61-40, NASA-Marshall Space Flight Center, Huntsville, Alabama, September 15, 1961.

18. E. Cagle, P. Youngblood, R. Boehme, S-46 Satellite, Vol. II of Summary Project Report, TN D-608, NASA-Marshall Space Flight Center, Huntsville, Alabama, April 1961.